1   **Future reduction of cold extremes over East Asia due to**

2   **thermodynamic and dynamic warming**

3   Donghuan Li[1, 3], Tianjun Zhou[2, 3, 5*], Youcun Qi[1, 3], Liwei Zou[2], Chao Li[4], Wenxia

4   Zhang[2], Xiaolong Chen[2]

5   *[1]Key Laboratory of Water Cycle and Related Land Surface Processes, Institute of Geographic*

6   *Sciences and Natural Resources Research, Chinese Academy of Sciences, Beijing, China*

7   *[2]LASG, Institute of Atmospheric Physics, Chinese Academy of Science, Beijing, China*

8   *[3]University of Chinese Academy of Sciences, Beijing, China*

9   *[4]Max Planck Institute for Meteorology, Hamburg, Germany*

10   *[5]CAS Center for Excellence in Tibetan Plateau Earth Sciences, Chinese Academy of Sciences*

11   *(CAS), Beijing, China*

13   **Corresponding author:**

14   Dr. Tianjun ZHOU

15   LASG, Institute of Atmospheric Physics

16   Chinese Academy of Sciences

17   Beijing 100029, China.

18   Phone: 86-10-8299-5279

19   Fax: 86-10-8299-5172

20   E-mail: *zhoutj@lasg.iap.ac.cn*

Abstract

Cold extremes have large impacts on human society. Understanding the physical processes dominating the changes of cold extremes is crucial for a reliable projection of future climate change. The observed cold extremes have decreased during the last several decades and this trend will continue under future global warming. Here, we quantitatively identify the contributions of dynamic (changes in large-scale atmospheric circulation) and thermodynamic (rising temperatures resulting from global warming) effects to East Asian cold extremes in the past several decades and in a future warm climate by using two sets of large ensemble simulations of climate models. We show that the dynamic component accounts for over 80% of the cold-month (coldest 5% boreal winter months) surface air temperature (SAT) anomaly in the past five decades. However, in a future warm climate, the thermodynamic change is the main contributor to the decreases in the intensity and occurrence probability of East Asian cold extremes, while the dynamic change is also contributive. The intensity of East Asian cold extremes will decrease by around 5℃ at the end of the 21st century, in which the thermodynamic (dynamic) change contributes approximately 75% (25%). The present-day (1986-2005) East Asian cold extremes will almost never occur after around 2035, and this will happen ten years later due solely to thermodynamic change. The upward trend of a positive Arctic Oscillation-like sea level pressure pattern dominates the changes in the dynamic component. The finding provides a useful reference for policymakers in climate change adaptation activities.

Keywords: East Asian cold extreme, dynamic adjustment, global warming

1 Introduction

Extreme events are widely concerning because of their high destructive power and great social impacts. Cold extremes have great impacts on agriculture, transportation, and people's health, and can even cripple power supplies and lead to rolling blackouts (Steponkus, 1979; Andreescu and Frost, 1998; Sheridan et al., 2015; Thornton et al., 2016). The global mean surface air temperature (SAT) has been increasing in the past century due to the increase of anthropogenic greenhouse gas concentration in the atmosphere (Jones et al., 2008; IPCC, 2021). While warm extremes continue to attract considerable attention from the scientific community and ordinary people (e.g. Alexander et al., 2006; Rahimzadeh et al., 2009; Donat et al., 2012; Sun et al., 2014; Ma et al., 2017b), the cold extremes have also gained wide attention (e.g. Overland et al., 2011; Mori et al., 2014; Li et al., 2015; McCusker et al., 2016; Sun et al., 2016; Trenary et al., 2016; Ma et al., 2018; Qian et al., 2018) due to the mid-latitude cold extremes happened in recent several years.

A strong cold surge related to the negative phase of the Arctic Oscillation (AO) and intensified Siberian High attacked North China during 6-8 January 2021 (Wang et al., 2021). The temperatures reached or broke the records in more than 50 cities and counties. Beijing experienced the third coldest day since 1951 on 7 January, with a daily minimum temperature of -19.6°C. (Wang et al., 2021; Zhou et al., 2022). The regional mean temperature in North China during 6-8 January 2021 was about 9°C lower than the average for the same period between the years 2001 and 2020. North America evidenced a widespread cold extreme in February 2021, which was caused by the

67 distorted and weakened polar vortex (Lee, 2021; Lu et al., 2021). The temperatures

68 were 15°C to 25°C lower than normal in large areas and caused huge impacts on the

69 energy supplies and transportation (Zhou et al., 2022). Cold extremes have occurred

70 from time to time under global warming in recent years. Will it continue to occur while

71 global warming continues in the future?

72   The model simulations indicate that the anthropogenic influences have reduced

73 the occurrence probability of cold extremes over eastern China with intensity stronger

74 than the record-breaking cold extreme (since modern meteorological observations

75 started in 1960) on 21-25 January 2016 (Qian et al., 2018). The wintertime East Asian

76 SAT is projected to increase significantly as a response to future global warming (IPCC,

77 2021). Cold months defined based on the 20th century will be rarer under future global

78 warming (Räisänen and Ylhäisi, 2011) and the future warming will continuously reduce

79 the intensity and occurrence probability of the cold extreme events (annual minimum

80 daily minimum temperature) over East Asia (Kharin et al., 2013; 2018).

81   Previous studies demonstrated that the SAT is influenced by both the dynamic

82 (changes in large-scale atmospheric circulation) and thermodynamic effects

83 (Thompson et al., 2009; Cattiaux et al., 2010; Wallace et al., 2012; Smoliak et al., 2015;

84 Deser et al., 2016). The dynamic effect, for example, the Arctic amplification, which

85 reduces the polar-to-equator temperature gradient, can further modify the atmospheric

86 circulation. There is a positive AO-like SLP (sea level pressure) changing pattern under

87 global warming (Fyfe et al., 1999; Yamaguchi and Noda, 2006; Kitoh, 2017) and the

88 East Asian winter monsoon will be weakened in the warmer future conditions according

89   to the multi-model simulations of the CMIP3 and CMIP5 models (Jiang and Tian, 2013;

90   Xu et al., 2016). However, there is a lack of quantitative research on the contributions

91   of the dynamic and thermodynamic effects to the future changes of the East Asian cold

92   extremes if the global mean SAT continues to increase.

93   The "dynamic adjustment" approach (Wallace et al., 2012; Smoliak et al., 2015;

94   Deser et al., 2016) has been proposed to divide the SAT anomaly into dynamic

95   component (solely associated with circulation changes) and thermodynamic component

96   (associated with thermodynamic processes). The dynamic adjustment of the North

97   Hemisphere SAT field based on SLP can be used to investigate both the short-term

98   climate fluctuations and long-term trends of SAT (Smoliak et al., 2015). Deser et al.

99   (2016) indicates that the internal circulation trends account for over 30% of the North

100   American wintertime warming trend in the past 50 years. The variability of circulation

101   plays a critical role in the evolution of the East Asian winter temperature trends during

102   1961-2018 and the internally induced dynamic component offsets the forced warming

103   by over 70% in northern East Asia over the time period of 1979–2018 (Gong et al.,

104   2019; 2021). The dynamic adjustment approach has also been used to investigate the

105   wintertime precipitation changes and summertime SAT changes over East Asia (e.g.,

106   Guo et al., 2019; Hu et al., 2019). However, these studies mainly focus on the mean

107   temperature and mean precipitation changes in the past several decades, very few

108   studies have quantified the contributions of the dynamic and thermodynamic effects to

109   the future changes of the East Asian cold extremes associated with global warming.

110   By using two sets of grand ensemble simulations combined with observational

data and reanalysis data, we aim to answer the following questions: (1) What are the relative contributions of the dynamic and thermodynamic effects to the East Asian cold extremes in the past several decades? (2) How will the intensity and occurrence probability of East Asian cold extremes change in the warmer future and what are the quantitative contributions of the dynamic and thermodynamic effects to the changes of East Asian cold extremes in the warmer future? (3) How will the circulation change in the warmer future and how will this change affect cold extremes in East Asia?

2 Data and Methodology

2.1 Model Data

The 100-member Grand Ensemble generated by the Max Planck Institute Earth System Model version 1.1 (MPI-GE; Maher et al., 2019) with horizontal resolution of 1.8°×1.8° and the 40-member Community Earth System Model Large Ensemble (CESM-LE; Kay et al., 2015) with horizontal resolution of 1°×1° are applied in this study to investigate the contributions of dynamic and thermodynamic components to the East Asian cold extremes in recent decades and the future warm climate. The historical simulations integrated from 1850 to 2005 in the MPI-GE and from 1920 to 2005 in the CESM-LE were driven by the observed forcings. The Representative Concentration Pathway 8.5 (RCP8.5) scenario simulations were performed from 2006 to 2099 in the MPI-GE and from 2006 to 2100 in the CESM-LE. In addition, the 2000-yr MPI pre-industrial (PiCTL) simulation and 1800-yr CESM PiCTL simulation are also used in this study. For more detailed information on the MPI-GE and the CESM-

LE, please refer to Maher et al. (2019) and Kay et al. (2015), respectively.

2.2 Observation Data

The following datasets are used in this study: (1) monthly mean SAT from the Climatic Research Unit (CRU) version 4 with a horizontal resolution of 0.5°×0.5° (Harris et al., 2014). (2) Monthly mean three-dimensional circulation fields derived from the 20th Century Reanalysis (20CR) version 2 with a horizontal resolution of 2°×2° (Compo et al., 2011). The time period for these two datasets used in this study is from 1920 to 2012.

2.3 Dynamic Adjustment Approach

The dynamic adjustment method presented by Deser et al. (2016) is based on the constructed circulation analogue using SLP. This method empirically divides SAT variability into a dynamic component (associated with atmospheric circulation changes) and a thermodynamic component (the residual part). The dynamic adjustment method is summarized below and please refer to Deser et al. (2016) for more details.

2.3.1   Application to the MPI-GE and CESM-LE

For a given "target" month and year (e.g. December 1990) in each ensemble member, we rank the 2000 (1800) December SLP fields in the PiCTL simulation by their similarity with the target SLP pattern according to Euclidean distance. From the 150 SLP fields with the smallest Euclidean distances, we randomly subsample 100 SLP fields to construct the best estimation of the target SLP pattern by linear combination. The same set of linear coefficients is applied to the accompanying SAT fields to obtain

153   the associated linear combination of SAT. We repeat the subsampling procedure 100

154   times and average the 100 linear combinations to derive the dynamically induced SAT

155   field in the target month. Deser et al. (2016) illustrate the importance of this iterative

156   random selection process and the reason for the repeated subsampling procedure is to

157   take into account the uncertainty related to internal thermodynamic variability and to

158   ensure the robustness of the results. We use the domain $15°\sim90°N$, $30°\sim180°E$ for the

159   SLP analogues. The sensitivity to the precise region used is small (Figures not shown;

160   e.g. within $\pm5°$ of latitude and $\pm10°$ of longitude). To test whether 150 selected SLP

161   fields are sufficient to estimate the target SLP, a sensitivity analysis is conducted on the

162   sample size of the selected closest fields. The findings suggest that there is no

163   significant difference when the number of selected fields exceeds 100.

164   The multi-member mean of the dynamic component is regarded as the forced

165   dynamic component and the internal dynamic component is obtained by subtracting the

166   forced part from the total dynamic component for each ensemble member.

167   Thermodynamic components are obtained as residuals (total minus dynamic) for both

168   forced and internal components.

169   **2.3.2 Application to the observation**

170   There is no PiCTL simulation in the observation. Therefore, before computing the

171   dynamic component of SAT, the quadratic trend of the SAT during 1920-2012 is first

172   subtracted to obtain SAT series without anthropogenic forcing. Similar to the

173   application to the model ensembles, for each month and year in the observation, 40 SLP

174 fields subsampled from 60 closest SLP fields are first selected (excluding the target

175 month). Then, dynamic adjustment procedure described in section 2.3.1 is applied to

176 derive the dynamically-induced SAT fields in the observation.

177   Different from model simulations, there is only one member in the observation,

178 we cannot separate the forced and internal parts by calculating the ensemble mean or

179 subtracting the ensemble mean. To obtain the internal dynamic contribution to the

180 observed SAT anomaly, a separate dynamic adjustment based on the internal component

181 of the observed SLP anomalies is performed. It is worth noting that, the internal

182 component of the observed SLP anomalies is obtained by subtracting the model

183 ensemble-mean SLP anomaly from the observed SLP anomaly at each time step.

184   After we get the internal dynamic component of SAT anomaly, the forced dynamic

185 component is calculated by subtracting the internal dynamic component from the total

186 dynamic component. Thermodynamic components are obtained as residuals (total

187 minus dynamic) for both forced and internal components.

188 **2.4 Baseline period and the study region**

189   The baseline period of 1986-2005 boreal winter is referred to as the historical

190 (present-day) climatology to investigate the SAT anomalies and contributions of

191 dynamic and thermodynamic effects to future changes of East Asian cold extremes. The

192 certain region (the black box in Figure 2) from 20°N to 55°N and from 105°E to 130°E

193 is regarded as East Asia in this study.

194 **2.5 The definitions of cold extreme and cold month**

The definition of East Asian cold extreme is as follows: in the models, the regional averaged monthly SAT anomaly of East Asia is firstly calculated. For a specific period, cold extremes are defined as the months in which the regional mean SAT is lower than the statistical 5th percentile of the climatological monthly SAT series during DJF in this time period. A month when a cold extreme happens is defined as a cold month. Similarly, the cold months in the observation are the 8 coldest months (5% of 150 winter months) during the 1962-2011 boreal winter (Table 1).

All the anomalies shown in this study are calculated relative to the climatological values of the 1986-2005 boreal winter unless mentioned otherwise. Student's t-test is applied to indicate the 5% significance level.

2.6 The intensity and occurrence probability ratio of cold extreme

The intensity of a cold extreme is the SAT deviation relative to the present-day boreal winter SAT climatology.

The occurrence probability ratio of the present-day cold extremes is calculated as follows (Ma et al., 2017a):

$$PR = \frac{P1}{P0} \tag{1}$$

where PR is the occurrence probability ratio. The value of $P0$ is 5%, and $P1$ is the probability of monthly SAT lower than the present-day cold extreme threshold in other time periods. For example, if the value of $P1$ is 2% during a future period, then the value of PR is 0.4. For the calculation of the occurrence probability ratio, we pull all the members together rather than calculate it for each member.

3 Results

3.1 Dynamic and thermodynamic processes to East Asian cold extremes in recent decades

The observed winter temperature in East Asia shows obvious variability during the 1962-2011 boreal winter (Figure 1a). According to the correlation coefficients calculated between each component of the SAT anomaly and the original SAT anomaly, the SAT variability is mainly caused by the dynamically induced internal component (Figure 1b-g). The fluctuations of forced dynamic and thermodynamic components are much smaller than those of internal dynamic and thermodynamic ones (Figure 1c, d, f and g). Internal variability is the main cause of cold extremes over East Asia in the past five decades (Figure 1).

The decomposition of the observed East Asian cold-month SAT anomalies during the 1962-2011 boreal winter is shown in Figure 2a-c. The SAT is significantly lower than the present-day winter SAT climatology (more than 3℃) across the East Asian landmass (Figure 2a). The decomposition of the SAT anomaly indicates that the cold extremes in recent decades are mainly caused by the dynamic component (Figure 2b and c). The dynamic component accounts for approximately 55% of the total East Asian cold-month SAT anomaly during the 1962-2011 boreal winter. Compared to cold extremes in the 1960s and 1970s, the percentage contribution of dynamic components to the cold extreme in January 2011 is higher (Table 1). The East Asian regional mean SAT anomaly in January 2011 is -3.47℃, in which, the dynamic component is -3.81℃,

accounting for up to 110% of the total SAT anomaly (Table 1). It is worth noting that these cold extremes are mainly caused by the internally generated components, and the forced dynamic component has shown little trend in the past five decades and has little contribution to the observed cold extremes (Figure 1c and d).

The two sets of large ensemble model simulations can generally capture the spatial distributions of total SAT anomaly and the dynamic component of cold extremes during 1962-2011 boreal winter (Figure 2d, e, g and h), with pattern correlation coefficients higher than 0.7 in both model ensembles. However, the thermodynamic component is much weaker in the model simulations than in the observation, especially in the northern parts of East Asia (Figure 2f and i). The dynamic component is the main contributor to the cold extremes, accounting for up to 85% and 82% of the total East Asian cold-month SAT anomaly during the 1962-2011 boreal winter in the MPI-GE and the CESM-LE, respectively. Compared with the observation, the contribution of the dynamic component to the cold extremes is larger in the two model ensembles (Figure 2). One possible reason is that there are only 8 cold extreme samples in the observation, and the relative contributions of dynamic and thermodynamic components cannot be fully reflected by these samples. Another possible reason may be the uncertainty of local thermodynamic processes (Röthlisberger and Papritz, 2023).

The results shown above indicate that the observed cold extremes in the past decades are mainly caused by the internal variability of atmospheric circulations. The cold extremes are often associated with strong East Asian winter monsoon flows, which are often accompanied by the blockings in the Urals and the intensified Siberian high

259 (Francis and Vavrus, 2012; Ma et al., 2018). The composite circulation anomalies in the

260 cold months during the 1962-2011 boreal winter are further investigated (Figure 3). A

261 ridge-trough pattern is seen over the Eurasian continent in the upper troposphere and

262 there is southeastward propagation of wave activity flux (Figure 3a). The westerlies are

263 weakened in the whole troposphere around 45°N~75°N, and there is an enhanced

264 meandering flow pattern (Figure 3b; Walsh, 2014; Simmonds, 2015; Ma et al., 2018).

265 The weakened westerlies may favor the blocking events, which have a strong

266 relationship with the cold extremes over East Asia (Luo et al., 2017). The surface

267 Siberian High is intensified, and low-level northerly winds lead cold Arctic air to spread

268 southward to East Asia (Figure 3c).

269 This typical type of circulation anomalies in cold months mentioned above are

270 also well captured in the MPI-GE and the CESM-LE (Figure 3d-f). Namely, there is a

271 ridge-trough pattern in the upper troposphere over the Eurasian continent and the

272 surface Siberian High is enhanced. The westerlies are weakened in the whole

273 troposphere and the cold air from the Arctic regions causes cold extremes over East

274 Asia.

275 **3.2 Dynamic and thermodynamic contributions to the projected changes in East**

276 **Asian cold extremes**

277 In the observations, the dynamic component is the main contributor to the East

278 Asian cold extremes in the past five decades. The human-induced global warming had

279 little effect on the changes in dynamically-induced SAT anomalies during 1962-2011

(Figure 1). How will the dynamic and thermodynamic effects contribute to the future changes in cold extremes over East Asia?

We first examine the changes in the intensity of East Asian cold extremes (Figure 4a and c). The SAT anomaly will continuously increase along with global warming under the RCP8.5 scenario. Compared with the present day, the East Asian regional mean cold-month SAT will increase by approximately 4.7°C at the end of the 21st century according to the best estimation of MPI-GE (Figure 4a). The large center is located in Northeast China, over 6°C (Figure 5a). The dynamic and thermodynamic components will also continually increase under the RCP8.5 scenario. It is worth noting that, the dynamic component explains a larger part of the total SAT anomaly in cold months before approximately 2040. Thereafter, the thermodynamic component is the main driver in both model ensembles (Figure 4a and c). The increases in the dynamic and thermodynamic components are approximately 1.3°C and 3.4°C at the end of the 21st century, respectively, in the MPI-GE (Figure 4a). Therefore, the contribution of the increase in dynamic component to the total SAT increase is 27%. The dynamic and thermodynamic components also increase faster in northern parts of East Asia than in other regions (Figure 5b and c). The faster increase of thermodynamic component in northern East Asia may be caused by the snow-albedo feedback (Fischer et al., 2011), while the reason for the faster increase in dynamic component in this region is that the influence of East Asian Winter Monsoon on northern East Asia is more evident than on other subregions (He et al., 2017). The results in the CESM-LE are generally consistent with those in the MPI-GE. The East Asian regional mean SAT anomalies in cold months

302   will increase by approximately 5.2°C at the end of the 21st century (Figure 4c). The

303   corresponding increases in the dynamic and thermodynamic components are 1.3°C and

304   3.9°C, respectively. Statistically, the contribution of the increase in dynamic component

305   to the total SAT increase is about 25%. From the perspective of spatial distribution, total

306   SAT and its dynamic and thermodynamic components show similar changing patterns

307   in the two sets of large ensemble model simulations, with large increases occurring in

308   northern parts of East Asia (Figure 5). However, there are some local differences

309   between the two models. Compared with MPI-GE, the end-of-the 21st-century increase

310   in cold-month regional mean SAT is approximately 0.5°C higher in CESM-LE,

311   primarily due to the thermodynamic component. The larger increase of thermodynamic

312   component in Northeast and Southeast China in CESM-LE than in MPI-GE may be

313   attributed to differences in thermal feedback processes, such as the snow-albedo

314   feedback and land-surface fluxes (Seneviratne et al., 2010; Fischer et al., 2011;

315   Röthlisberger and Papritz, 2023).

316   We extend the analysis from the changes in the intensity of cold extremes to the

317   changes in the occurrence probability ratio of the present-day cold extremes in the

318   future warm climate (Figure 4b). The 20-year running occurrence probability ratio of

319   the present-day cold extremes will rapidly decrease under the RCP8.5 scenario in both

320   sets of the large ensemble model simulations. In the MPI-GE, the occurrence

321   probability ratio of the present-day cold extremes will decrease to 0.05 in the period

322   from 2036 to 2055 (Figure 4b), which means the present-day cold extremes will almost

323   never occur after 2036. We isolate the dynamic and thermodynamic contributions to the

changes in the occurrence probability ratio of the present-day cold extremes. If we hold

the dynamic component constant at the present-day level, and allow the thermodynamic

component to evolve according to the model projection, the year when the occurrence

probability ratio of the present-day cold extremes will decrease to 0.05 is approximately

ten years later than the time mentioned above (Figure 4b). Correspondingly, if we hold

the thermodynamic component constant at the present-day level, and allow the dynamic

component to evolve according to the model projection, the occurrence probability ratio

of the present-day cold extremes will decrease to about 0.3 at the end of the 21st century.

From the perspective of spatial distribution, the occurrence probability ratio of the

present-day cold extremes will be decreased to 0.05 before 2040 in parts of southeastern

China, northeastern China and the Korean Peninsula (Figure 6a). The results in the

CESM-LE are generally consistent with those in the MPI-GE (Figures 4d and 6b). The

occurrence probability ratio of the present-day cold extremes will decrease to 0.05 in

2035-2054 (Figure 4d) and the occurrence probability ratio also decreases faster in

southeastern China, parts of northeastern China and the southern Korean Peninsula

(Figure 6b). Different from the MPI-GE, the occurrence probability ratio of the present-

day cold extremes will decrease to 0.05 after 2060 in parts of North China in the CESM-

LE (Figure 6b).

The thermodynamic component dominates the future decrease in the intensity and

occurrence probability of East Asian cold extremes, while the dynamic component is

also contributive. Dynamic change accounts for approximately one-quarter of the total

change in the intensity of cold extremes by the end of the 21st century. We further

examine the changes in SLP anomalies associated with East Asian cold extremes (Figures 7 and 8).

Similar to the previous studies (Fyfe et al., 1999; Cai et al., 2017; Kitoh, 2017), the projected changes in SLP exhibit a positive AO-like pattern, especially in MPI-GE (Figure 7). The pattern correlation coefficients between the SLP changing patterns and the positive phase of AO in MPI-GE and CESM-LE are approximately 0.7 and 0.4, respectively (Figure 7a and c). The winter-mean SLP will be reduced in the Arctic regions and enhanced in the mid-latitude regions. The AO shows a highly positive correlation with the winter SAT anomaly over East Asia, especially the northern part, and the positive phase of AO is favorable for warm winter over East Asia (Gong et al., 2019; Wang et al., 2019). The SLP changing patterns in cold months (Figure 7b and d) are similar to those in winter mean (Figure 7a and c), and this is possibly the reason for the positive contribution of dynamic effects to the increase in SAT anomaly in cold months. We also construct the changes in the dynamic component of SLP (Figure 8). Changes in the dynamic component of SLP also corroborate that the circulation changes are not favorable for the occurrence of East Asian cold extremes. There are some differences in the SLP changing patterns between the two model ensembles, particularly during cold extremes over the Eurasian region. This could be one of the possible reasons for the differences in local dynamic changes in the two model ensembles.

4 Summary and Discussion

4.1 Summary

367   Based on the dynamic adjustment approach, we utilized two sets of large ensemble

368 model simulations in the MPI-GE and CESM-LE to investigate the contributions of the

369 background warming (thermodynamic effect) and circulation changes (dynamic effect)

370 to the East Asian cold extremes. The contributions of the two components to the East

371 Asian cold extremes are quantitatively evaluated in the recent decades and under future

372 warming. The main conclusions are summarized as follows.

373 (1) The observed cold extremes in the past decades are mainly caused by the internal

374   variability of atmospheric circulations. Compared to cold extremes in the 1960s and

375   1970s, the percentage contribution of dynamic component to the cold extreme in

376   recent years is higher. Both MPI-GE and the CESM-LE are consistent in revealing

377   the typical circulation anomalies associated with the East Asian cold extremes.

378   Compared with the observation, the contribution of the dynamic component to the

379   cold extremes is more evident in the two model ensembles, and the dynamic

380   component accounts for more than 80% of the total cold-month SAT anomalies in

381   the past five decades.

382 (2) In the future warm climate, the decreases in the intensity and occurrence probability

383   of East Asian cold extremes are dominated by thermodynamic component, while

384   the dynamic component is also contributive. According to MPI-GE and CESM-LE,

385   compared with the present day, the mean intensity of the East Asian cold extremes

386   will decrease by approximately 5°C at the end of the 21st century under the RCP8.5

387   scenario and the dynamic component contributes to a quarter of this decrease. The

388   occurrence probability ratio of the present-day cold extremes will almost never

occur after around 2035, and if we hold the dynamic component constant at the present-day level, this will happen approximately 10 years later.

(3) Positive AO-like sea level pressure pattern upward trend is projected in both of the model ensembles, which is unfavorable to the occurrence of East Asian cold extremes. There are a few differences between the two ensemble projections, particularly in the Eurasian region during cold extremes, and this could be one of the possible reasons for the local differences of dynamic components in the two model ensembles.

4.2 Discussion

Substantial efforts have been devoted so far to understanding the response of climate extremes to global warming (e.g. Alexander et al., 2006; Sanderson et al., 2017; Zhang et al., 2018; AghaKouchak et al., 2020; Li et al., 2021), as well as their physical mechanisms (Cattiaux et al., 2010; Peing and Magnusdottir, 2014; Westra et al., 2014; Boschat et al., 2015; Horton et al., 2015; Qian et al., 2018). In particular, the thermodynamic processes (i.e., direct results of global warming) of changes in climate extremes have been well demonstrated. However, it remains ambiguous regarding how the dynamic processes will change under global warming, which is an important source of projection uncertainty for climate extremes (Shepherd, 2014; Norris et al., 2019). Hence, it is of vital importance to understand the dynamic changes of climate extremes, in order to improve the reliability of extreme climate projections.

In this study, we used two sets of large ensemble simulation data and a dynamic

410   adjust method to investigate the future change of cold extremes in East Asia, with a

411   focus on understanding the thermodynamic and dynamic processes. Our results

412   consistently show that the thermodynamic process is the dominant factor of future

413   changes in East Asian cold extreme, with the contribution of dynamic process

414   accounting for approximately one-quarter of the total change. In addition, the change

415   in the dynamic component is attributed to the upward trend of a positive AO-like sea

416   level pressure pattern, and this has been supported by previous studies (Fyfe et al., 1999;

417   Cai et al, 2017; Kitoh, 2017).

418   AO is the main circulation mode in the non-tropical regions of the Northern

419   Hemisphere in winter (Thompson and Wallace, 1998), and has a significant impact on

420   the winter climate in East Asia (Gong et al., 2001). However, it is worth noting that

421   future winter temperature changes in East Asia may also be impacted by other large-

422   scale circulation factors (Zhou et al., 2007; Cheung et al., 2012; He and Wang, 2013).

423   The quantitative impacts of potential future changes of different circulation factors on

424   cold extremes in East Asia remain unclear and require further investigation in future

425   research.

Data availability

The MPI-GE experiment products can be downloaded from https://esgf-data.dkrz.de/search/mpi-ge/. The specific experiments or variables can be selected through the navigation bar on the left-hand side. The monthly sea level pressure (psl), surface air temperature (tas), three-dimensional wind field (ua, va, wap), and geopotential height (zg) from the piControl, historical and rcp85 experiments are used in this work.

The CESM-LE experiment products can be downloaded from https://www.earthsystemgrid.org/dataset/ucar.cgd.ccsm4.cesmLE.html.

Author contribution

TJZ designed the study. DHL performed the data analysis, produced the figures and wrote the manuscript draft. YCQ and CL collected the datasets. LWZ, WXZ and XLC contributed to the analysis methods. All the authors contributed to the discussion, writing, and editing of the manuscript.

Competing interests

The authors declare that they have no competing interests.

Acknowledgements

This work is jointly supported by the National Natural Science Foundation of China (Grant Nos. 42105031, 41988101).

References

AghaKouchak, A., Chiang, F., Huning, L. S., Love, C. A., Mallakpour, I., Mazdiyasni, O., ... & Sadegh, M. (2020). Climate extremes and compound hazards in a warming world. Annual Review of Earth and Planetary Sciences, 48, 519-548. https://doi.org/10.1146/annurev-earth-071719- 055228.

Alexander, L. V., Zhang, X., Peterson, T. C., Caesar, J., Gleason, B., Klein Tank, A. M. G., ... & Vazquez‑Aguirre, J. L. (2006). Global observed changes in daily climate extremes of temperature and precipitation. Journal of Geophysical Research: Atmospheres, 111(D5). https://doi.org/10.1029/2005JD006290

Andreescu, M. P., & Frost, D. B. (1998). Weather and traffic accidents in Montreal, Canada. Climate research, 9(3), 225-230. https://doi.org/10.3354/cr009225

Boschat, G., Pezza, A., Simmonds, I., Perkins, S., Cowan, T., & Purich, A. (2015). Large scale and sub-regional connections in the lead up to summer heat wave and extreme rainfall events in eastern Australia. Climate Dynamics, 44, 1823-1840. https://doi.org/10.1007/s00382-014-2214-5.

Cai, W., Li, K., Liao, H., Wang, H., & Wu, L. (2017). Weather conditions conducive to Beijing severe haze more frequent under climate change. Nature Climate Change, 7(4), 257-262. https://doi.org/10.1038/nclimate3249

Cattiaux, J., Vautard, R., Cassou, C., Yiou, P., Masson‑Delmotte, V., & Codron, F. (2010). Winter 2010 in Europe: A cold extreme in a warming climate. Geophysical Research Letters, 37(20). https://doi.org/10.1029/2010GL044613

470 Cheung, H. N., Zhou, W., Mok, H. Y., & Wu, M. C. (2012). Relationship between Ural–

471   Siberian blocking and the East Asian winter monsoon in relation to the Arctic

472   Oscillation and the El Niño–Southern Oscillation. Journal of Climate, 25(12),

473   4242-4257. https://doi.org/10.1175/JCLI-D-11-00225.1

474 Compo, G. P., Whitaker, J. S., Sardeshmukh, P. D., Matsui, N., Allan, R. J., Yin, X., ...

475   & Worley, S. J. (2011). The twentieth century reanalysis project. Quarterly Journal

476   of the Royal Meteorological Society, 137(654), 1-28.

477   https://doi.org/10.1002/qj.776

478 Deser, C., Terray, L., & Phillips, A. S. (2016). Forced and internal components of winter

479   air temperature trends over North America during the past 50 years: Mechanisms

480   and implications. Journal of Climate, 29(6), 2237-2258.

481   https://doi.org/10.1175/JCLI-D-15-0304.1

482 Donat, M. G., & Alexander, L. V. (2012). The shifting probability distribution of global

483   daytime and night‐time temperatures. Geophysical Research Letters, 39(14).

484   https://doi.org/10.1029/2012GL052459

485 Fischer, E. M., Lawrence, D. M., & Sanderson, B. M. (2011). Quantifying uncertainties

486   in projections of extremes—A perturbed land surface parameter

487   experiment. Climate Dynamics, 37, 1381-1398.

488 Francis, J. A., & Vavrus, S. J. (2012). Evidence linking Arctic amplification to extreme

489   weather in mid‐latitudes. Geophysical research letters, 39(6).

Fyfe, J. C., Boer, G. J., & Flato, G. M. (1999). The Arctic and Antarctic Oscillations and their projected changes under global warming. Geophysical Research Letters, 26(11), 1601-1604. https://doi.org/10.1029/1999GL900317

Gong, D. Y., Wang, S. W., & Zhu, J. H. (2001). East Asian winter monsoon and Arctic oscillation. Geophysical Research Letters, 28(10), 2073-2076. https://doi.org/10.1029/2000GL012311

Gong, H., Wang, L., Chen, W., & Wu, R. (2019). Attribution of the East Asian winter temperature trends during 1979–2018: Role of external forcing and internal variability. Geophysical Research Letters, 46(19), 10874-10881. https://doi.org/10.1029/2019GL084154

Gong, H., Wang, L., Chen, W., & Wu, R. (2021). Evolution of the East Asian winter land temperature trends during 1961–2018: role of internal variability and external forcing. Environmental Research Letters, 16(2), 024015. doi: 10.1088/1748-9326/abd586

Guo, R., Deser, C., Terray, L., & Lehner, F. (2019). Human influence on winter precipitation trends (1921–2015) over North America and Eurasia revealed by dynamical adjustment. Geophysical Research Letters, 46(6), 3426-3434. https://doi.org/10.1029/2018GL081316

Haarsma, R. J., Selten, F., Hurk, B. V., Hazeleger, W., & Wang, X. (2009). Drier Mediterranean soils due to greenhouse warming bring easterly winds over summertime central Europe. Geophysical research letters, 36(4). https://doi.org/10.1029/2008GL036617

Harris, I. P. D. J., Jones, P. D., Osborn, T. J., & Lister, D. H. (2014). Updated high‐resolution grids of monthly climatic observations–the CRU TS3. 10 Dataset. International journal of climatology, 34(3), 623-642. https://doi.org/10.1002/joc.3711

He, S., & Wang, H. (2013). Oscillating relationship between the East Asian winter monsoon and ENSO. Journal of Climate, 26(24), 9819-9838. https://doi.org/10.1175/JCLI-D-13-00174.1

He, S., Gao, Y., Li, F., Wang, H., & He, Y. (2017). Impact of Arctic Oscillation on the East Asian climate: A review. Earth-Science Reviews, 164, 48-62.

Horton, D. E., Johnson, N. C., Singh, D., Swain, D. L., Rajaratnam, B., & Diffenbaugh, N. S. (2015). Contribution of changes in atmospheric circulation patterns to extreme temperature trends. Nature, 522(7557), 465-469. https://doi.org/10.1038/nature14550

Hu, K., Huang, G., & Xie, S. P. (2019). Assessing the internal variability in multi-decadal trends of summer surface air temperature over East Asia with a large ensemble of GCM simulations. Climate Dynamics, 52(9), 6229-6242. https://doi.org/10.1007/s00382-018-4503-x

IPCC. (2021). Climate Change 2021. The Physical Science Basis. Contribution of Working Group I to the Sixth Assessment Report of the Intergovernmental Panel on Climate Change [Masson-Delmotte, V., P. Zhai, A. Pirani, S.L. Connors, C. Péan, S. Berger, N. Caud, Y. Chen, L. Goldfarb, M.I. Gomis, M. Huang, K. Leitzell, E. Lonnoy, J.B.R. Matthews, T.K. Maycock, T. Waterfield, O. Yelekçi, R. Yu, and

B. Zhou (eds.)]. Cambridge University Press, Cambridge, United Kingdom and New York, NY, USA, 2391 pp. doi:10.1017/9781009157896.

Jiang, D., & Tian, Z. (2013). East Asian monsoon change for the 21st century: Results of CMIP3 and CMIP5 models. Chinese Science Bulletin, 58(12), 1427-1435. https://doi.org/10.1007/s11434-012-5533-0

Jones, G. S., Stott, P. A., & Christidis, N. (2008). Human contribution to rapidly increasing frequency of very warm Northern Hemisphere summers. Journal of Geophysical Research: Atmospheres, 113(D2). https://doi.org/10.1029/2007JD008914

Kay, J. E., Deser, C., Phillips, A., Mai, A., Hannay, C., Strand, G., ... & Vertenstein, M. (2015). The Community Earth System Model (CESM) large ensemble project: A community resource for studying climate change in the presence of internal climate variability. Bulletin of the American Meteorological Society, 96(8), 1333-1349. https://doi.org/10.1175/BAMS-D-13-00255.1

Kharin, V. V., Flato, G. M., Zhang, X., Gillett, N. P., Zwiers, F., & Anderson, K. J. (2018). Risks from climate extremes change differently from 1.5 C to 2.0 C depending on rarity. Earth's Future, 6(5), 704-715. https://doi.org/10.1002/2018EF000813

Kharin, V. V., Zwiers, F. W., Zhang, X., & Wehner, M. (2013). Changes in temperature and precipitation extremes in the CMIP5 ensemble. Climatic change, 119(2), 345-357. https://doi.org/10.1007/s10584-013-0705-8

Kitoh, A. (2017). The Asian Monsoon and its Future Change in Climate Models: A Review. Journal of the Meteorological Society of Japan, 95(1): 7-33. https://doi.org/10.2151/jmsj.2017-002

Lee, S. H. (2021). The January 2021 sudden stratospheric warming. Weather, 76(4), 135-136. https://doi.org/10.1002/wea.3966

Li, C., Stevens, B., & Marotzke, J. (2015). Eurasian winter cooling in the warming hiatus of 1998–2012. Geophysical Research Letters, 42(19), 8131-8139. https://doi.org/10.1002/2015GL065327

Li, C., Zwiers, F., Zhang, X., Li, G., Sun, Y., & Wehner, M. (2021). Changes in annual extremes of daily temperature and precipitation in CMIP6 models. Journal of Climate, 34(9), 3441-3460. https://doi.org/10.1175/JCLI-D-19-1013.1

Lu, Q., Rao, J., Liang, Z., Guo, D., Luo, J., Liu, S., ... & Wang, T. (2021). The sudden stratospheric warming in January 2021. Environmental Research Letters, 16(8), 084029. doi: 10.1088/1748-9326/ac12f4

Luo, D., Yao, Y., Dai, A., Simmonds, I., & Zhong, L. (2017). Increased quasi stationarity and persistence of winter Ural blocking and Eurasian extreme cold events in response to Arctic warming. Part II: A theoretical explanation. Journal of Climate, 30(10), 3569-3587.

Ma, S., Zhou, T., Angélil, O., & Shiogama, H. (2017a). Increased chances of drought in southeastern periphery of the Tibetan Plateau induced by anthropogenic warming. Journal of Climate, 30(16), 6543-6560. https://doi.org/10.1175/JCLI-D-16-0636.1

Ma, S., Zhou, T., Stone, D. A., Angélil, O., & Shiogama, H. (2017b). Attribution of the July–August 2013 heat event in central and eastern China to anthropogenic greenhouse gas emissions. Environmental Research Letters, 12(5), 054020. doi: 10.1088/1748-9326/aa69d2

Ma, S., Zhu, C., Liu, B., Zhou, T., Ding, Y., & Orsolini, Y. J. (2018). Polarized response of East Asian winter temperature extremes in the era of Arctic warming. Journal of Climate, 31(14), 5543-5557. https://doi.org/10.1175/JCLI-D-17-0463.1

Maher, N., Milinski, S., Suarez‐Gutierrez, L., Botzet, M., Dobrynin, M., Kornblueh, L., ... & Marotzke, J. (2019). The Max Planck Institute Grand Ensemble: enablingthe exploration of climate system variability. Journal of Advances in Modeling Earth Systems, 11(7), 2050-2069. https://doi.org/10.1029/2019MS001639

McCusker, K. E., Fyfe, J. C., & Sigmond, M. (2016). Twenty-five winters of unexpected Eurasian cooling unlikely due to Arctic sea-ice loss. Nature Geoscience, 9(11), 838-842. https://doi.org/10.1038/ngeo2820

Mori, M., Watanabe, M., Shiogama, H., Inoue, J., & Kimoto, M. (2014). Robust Arctic sea-ice influence on the frequent Eurasian cold winters in past decades. Nature Geoscience, 7(12), 869-873. https://doi.org/10.1038/ngeo2277

Norris, J., Chen, G., & Neelin, J. D. (2019). Thermodynamic versus dynamic controls on extreme precipitation in a warming climate from the Community Earth System Model Large Ensemble. Journal of Climate, 32(4), 1025-1045. https://doi.org/10.1175/jcli-d-18-0302.1

Overland, J. E., Wood, K. R., & Wang, M. (2011). Warm Arctic—cold continents: climate impacts of the newly open Arctic Sea. Polar Research, 30(1), 15787. https://doi.org/10.3402/polar.v30i0.15787

Peings, Y., & Magnusdottir, G. (2014). Response of the wintertime Northern Hemisphere atmospheric circulation to current and projected Arctic sea ice decline: A numerical study with CAM5. Journal of Climate, 27(1), 244-264. https://doi.org/10.1175/JCLI-D-13-00272.1

Qian, C., Wang, J., Dong, S., Yin, H., Burke, C., Ciavarella, A., ... & Tett, S. F. (2018). Human Influence on the Record-breaking Cold Event in January of 2016 in Eastern China. [in "Explaining Extreme Events of 2016 from a Climate Perspective"]. Bulletin of the American Meteorological Society, 99(1), S118-S122. https://doi.org/10.1175/BAMS-D-17-0095.1

Rahimzadeh, F., Asgari, A., & Fattahi, E. (2009). Variability of extreme temperature and precipitation in Iran during recent decades. International Journal of Climatology: A Journal of the Royal Meteorological Society, 29(3), 329-343. https://doi.org/10.1002/joc.1739

Räisänen, J., & Ylhäisi, J. S. (2011). Cold months in a warming climate. Geophysical Research Letters, 38(22). https://doi.org/10.1029/2011GL049758

Röthlisberger, M., & Papritz, L. (2023). A global quantification of the physical processes leading to near‐surface cold extremes. Geophysical Research Letters, 50(5), e2022GL101670.

620 Sanderson, B. M., Xu, Y., Tebaldi, C., Wehner, M., O'Neill, B., Jahn, A., ... & Lamarque,

621   J. F. (2017). Community climate simulations to assess avoided impacts in 1.5 and

622   2 C futures. Earth System Dynamics, 8(3), 827-847. https://doi.org/10.5194/esd-

623   8-827-2017

624 Seneviratne, S. I., Corti, T., Davin, E. L., Hirschi, M., Jaeger, E. B., Lehner, I., ... &

625   Teuling, A. J. (2010). Investigating soil moisture–climate interactions in a

626   changing climate: A review. Earth-Science Reviews, 99(3-4), 125-161.

627 Shepherd, T. G. (2014). Atmospheric circulation as a source of uncertainty in climate

628   change projections. Nature Geoscience, 7(10), 703-708.

629   https://doi.org/10.1038/ngeo2253

630 Sheridan, S. C., & Allen, M. J. (2015). Changes in the frequency and intensity of

631   extreme temperature events and human health concerns. Current Climate Change

632   Reports, 1(3), 155-162. https://doi.org/10.1007/s40641-015-0017-3

633 Smoliak, B. V., Wallace, J. M., Lin, P., & Fu, Q. (2015). Dynamical adjustment of the

634   Northern Hemisphere surface air temperature field: Methodology and application

635   to observations. Journal of Climate, 28(4), 1613-1629.

636   https://doi.org/10.1175/JCLI-D-14-00111.1

637 Steponkus, P. L. (1979). Cold hardiness and freezing injury of agronomic crops.

638   Advances in Agronomy, 30, 51-98. https://doi.org/10.1016/S0065-

639   2113(08)60703-8

Sun, L., Perlwitz, J., & Hoerling, M. (2016). What caused the recent "Warm Arctic, Cold Continents" trend pattern in winter temperatures?. Geophysical Research Letters, 43(10), 5345-5352. https://doi.org/10.1002/2016GL069024

Sun, Y., Zhang, X., Zwiers, F. W., Song, L., Wan, H., Hu, T., ... & Ren, G. (2014). Rapid increase in the risk of extreme summer heat in Eastern China. Nature Climate Change, 4(12), 1082-1085. https://doi.org/10.1038/nclimate2410

Thompson, D. W., & Wallace, J. M. (1998). The Arctic Oscillation signature in the wintertime geopotential height and temperature fields. Geophysical research letters, 25(9), 1297-1300. https://doi.org/10.1029/98GL00950

Thompson, D. W., Wallace, J. M., Jones, P. D., & Kennedy, J. J. (2009). Identifying signatures of natural climate variability in time series of global-mean surface temperature: Methodology and insights. Journal of Climate, 22(22), 6120-6141. https://doi.org/10.1175/2009JCLI3089.1

Thornton, H. E., Hoskins, B. J., & Scaife, A. A. (2016). The role of temperature in the variability and extremes of electricity and gas demand in Great Britain. Environmental Research Letters, 11(11), 114015. doi: 10.1088/1748-9326/11/11/114015

Trenary, L., DelSole, T., Tippett, M. K., & Doty B. (2016). Extreme Eastern US Winter of 2015 Not Symptomatic of Climate Change [in "Explaining Extreme Events of 2016 from a Climate Perspective"]. Bulletin of the American Meteorological Society, 97(12), S31-S35. doi: 10.1175/BAMS-D-16-0156.1

661   Wallace, J. M., Fu, Q., Smoliak, B. V., Lin, P., & Johanson, C. M. (2012). Simulated

662   versus observed patterns of warming over the extratropical Northern Hemisphere

663   continents during the cold season. Proceedings of the National Academy of

664   Sciences, 109(36), 14337-14342. https://doi.org/10.1073/pnas.1204875109

665   Walsh, J. E. (2014). Intensified warming of the Arctic: Causes and impacts on middle

666   latitudes. Global and Planetary Change, 117, 52-63.

667   Wang, C., Yao, Y., Wang, H., Sun, X., & Zheng, J. (2021). The 2020 summer floods and

668   2020/21 winter extreme cold surges in China and the 2020 typhoon season in the

669   western North Pacific. Advances in Atmospheric Sciences. 38, 896 – 904.

670   https://doi.org/10.1007/s00376-021-1094-y

671   Wang, L., Deng, A., & Huang, R. (2019). Wintertime internal climate variability over

672   Eurasia in the CESM large ensemble. Climate dynamics, 52(11), 6735-6748.

673   https://doi.org/10.1007/s00382-018-4542-3

674   Westra, S., Fowler, H. J., Evans, J. P., Alexander, L. V., Berg, P., Johnson, F., ... &

675   Roberts, N. (2014). Future changes to the intensity and frequency of short‐

676   duration extreme rainfall. Reviews of Geophysics, 52(3), 522-555.

677   https://doi.org/10.1002/2014RG000464

678   Xu, M., Xu, H., & Ma, J. (2016). Responses of the East Asian winter monsoon to global

679   warming in CMIP5 models. International Journal of Climatology, 36(5), 2139-

680   2155. https://doi.org/10.1002/joc.4480

681 Yamaguchi, K., & Noda, A. (2006). Global warming patterns over the North Pacific:

682 ENSO versus AO. Journal of the Meteorological Society of Japan. Ser. II, 84(1),

683 221-241. https://doi.org/10.2151/jmsj.84.221

684 Zhang, W., Zhou, T., Zou, L., Zhang, L., & Chen, X. (2018). Reduced exposure to

685 extreme precipitation from 0.5C less warming in global land monsoon regions.

686 Nature Communications, 9(1), 3153. https://doi.org/10.1038/s41467- 018-05633-

687 3

688 Zhou, T., Zhang, W., Zhang, L., Clark, R., Qian, C., Zhang, Q., ... & Zhang, X. (2022).

689 2021: A Year of Unprecedented Climate Extremes in Eastern Asia, North America,

690 and Europe. Advances in Atmospheric Sciences. 39, 1598 – 1607.

691 https://doi.org/10.1007/s00376-022-2063-9

692 Zhou, W., Li, C., & Wang, X. (2007). Possible connection between Pacific oceanic

693 interdecadal pathway and East Asian winter monsoon. Geophysical Research

694 Letters, 34(1). https://doi.org/10.1029/2006GL027809

695

696   **Table 1** The list of observed cold months in period of 1962-2011 boreal winter.

Time (Year Month)	Total(°C)	Dynamic(°C)	Thermodynamic(°C)	Dynamic ratio (%)
196402	-5.63	-3.30	-2.33	58.6
196902	-5.02	-2.77	-2.25	55.1
197701	-4.51	-2.52	-1.98	56.0
196802	-4.35	-1.16	-3.19	26.6
196712	-4.01	-2.02	-2.00	50.3
201101	-3.47	-3.81	0.34	109.9
197202	-3.39	-0.45	-2.93	13.4
196612	-3.30	-2.55	-0.75	77.1

697

698
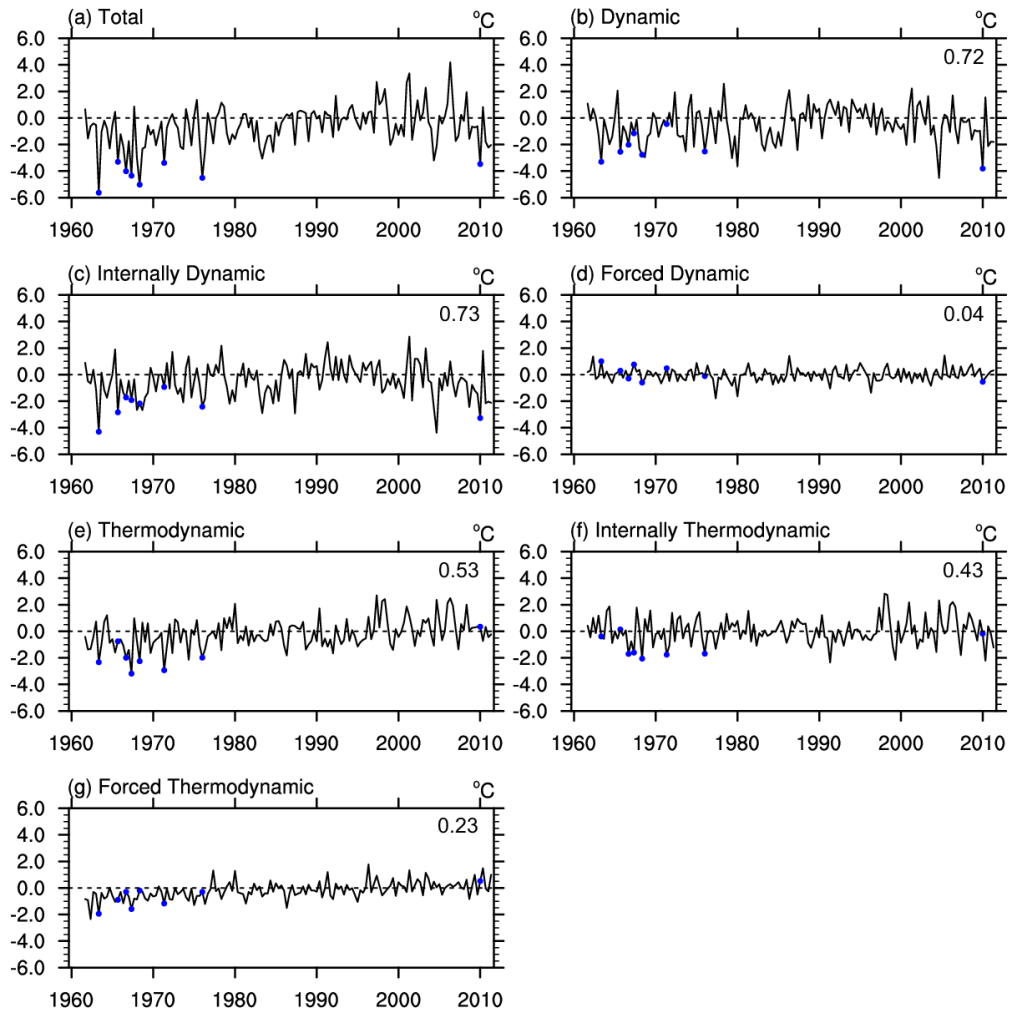
Figure 1 Time series decomposition of winter monthly surface air temperature (SAT) anomalies averaged over East Asia (20°N-55°N and from 105°E-130°E) from the observation into internal, forced, dynamic and thermodynamic components: (a) total, (b) dynamic, (c) internally dynamic, (d) forced dynamic and (e) thermodynamic components. The blue dots represent the cold months in the period of 1962-2011 boreal winter. The numbers in the upper right corner of subplots (b) to (g) represent the correlation coefficient between each component of SAT anomaly and the original SAT anomaly shows in subplot (a).
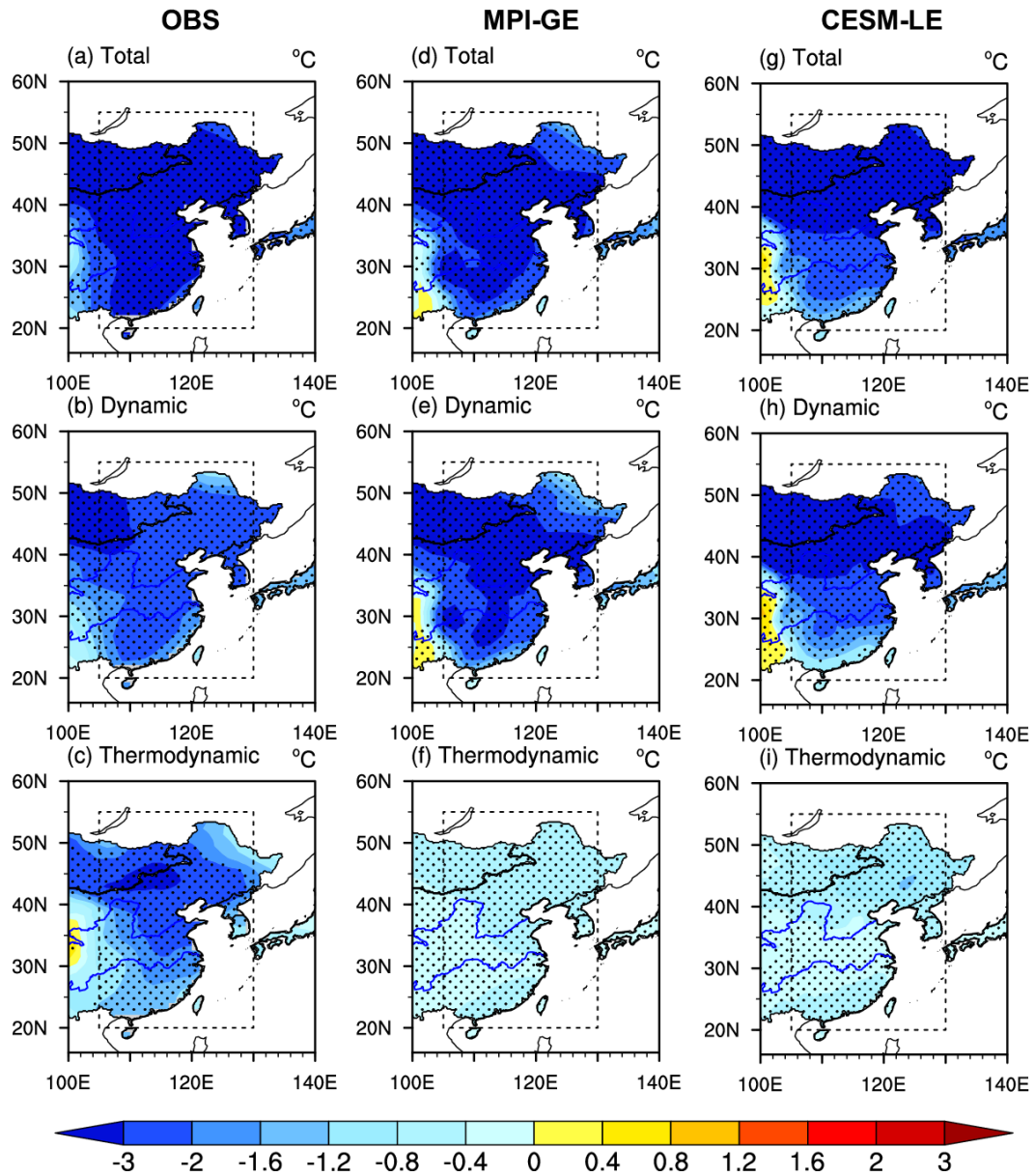
Figure 2 The composites of the cold-month SAT anomaly (relative to the 1986-2005

boreal winter climatology) in the observation during the period of 1962-2011 boreal

winter: (a) total, (b) dynamically-induced and (c) thermodynamically-induced. The

subplots (d)-(f) and (g)-(i) correspond to subplots (a)-(c), but for the results in the MPI-

GE and the CESM-LE, respectively. The dotted areas are statistically significant at the

5% level according to Student's t test. The cold months are defined as months in which

SAT is lower than the statistical 5th percentile of all the monthly SAT samples during

715   1962-2011 boreal winter.
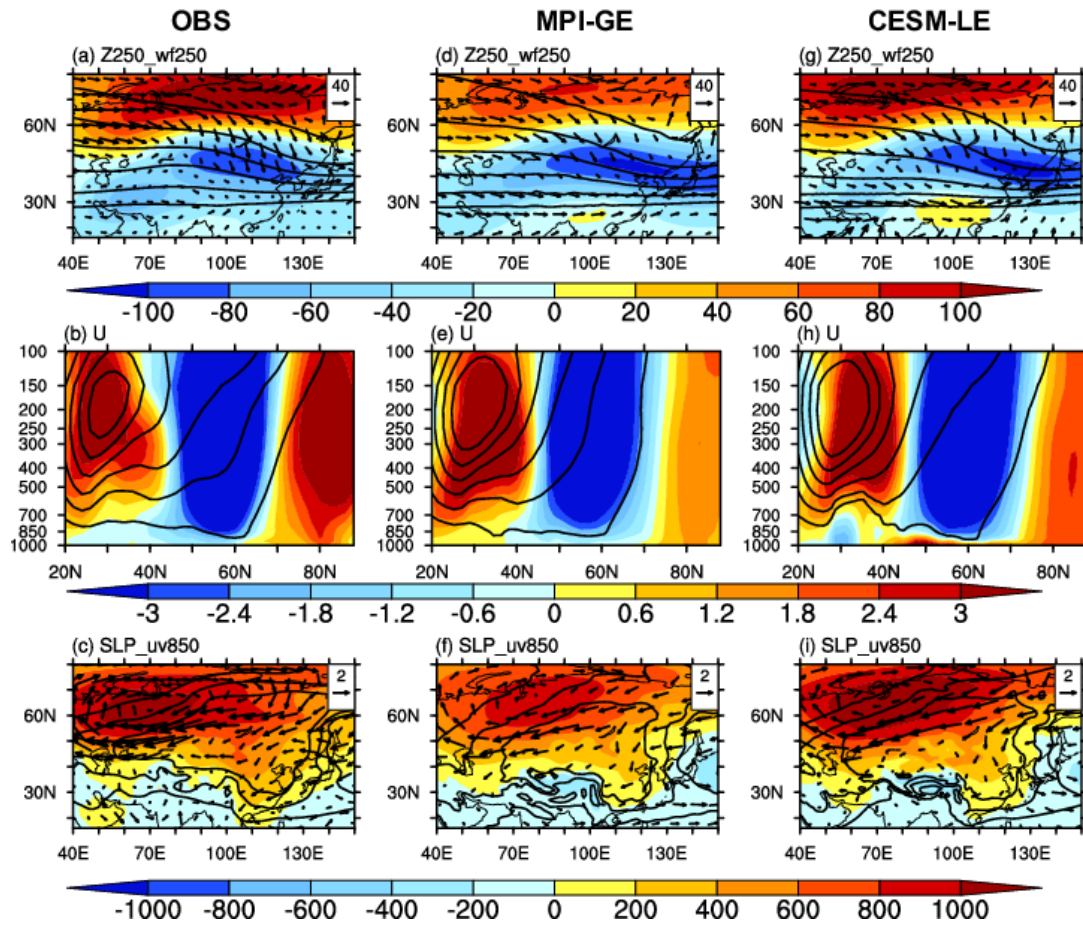
Figure 3 Observed composite circulation anomalies (relative to the 1986-2005 boreal

winter climatology) for East Asian cold extremes during the period of 1962-2011 boreal

winter: (a) Geopotential height (shading; unit: m) and horizontal components of the

wave activity flux ($m^2 s^{-2}$) at 250-hPa. (b) Zonal mean zonal wind over the vertical cross

section (zonally averaged over 70-120°E; unit: m s^{-1};). (c) Sea level pressure (shading;

unit: Pa) and horizontal wind at 850-hPa (m s^{-1}). The contours in subplots (a)-(c)

represent the 1986-2005 boreal winter climatology of geopotential height at 250-hPa,

zonal mean zonal wind over the vertical cross section, and sea level pressure,

respectively. Subplots (d)-(f) and (g)-(i) correspond to subplots (a)-(c), but for the

results in the MPI-GE and the CESM-LE, respectively.
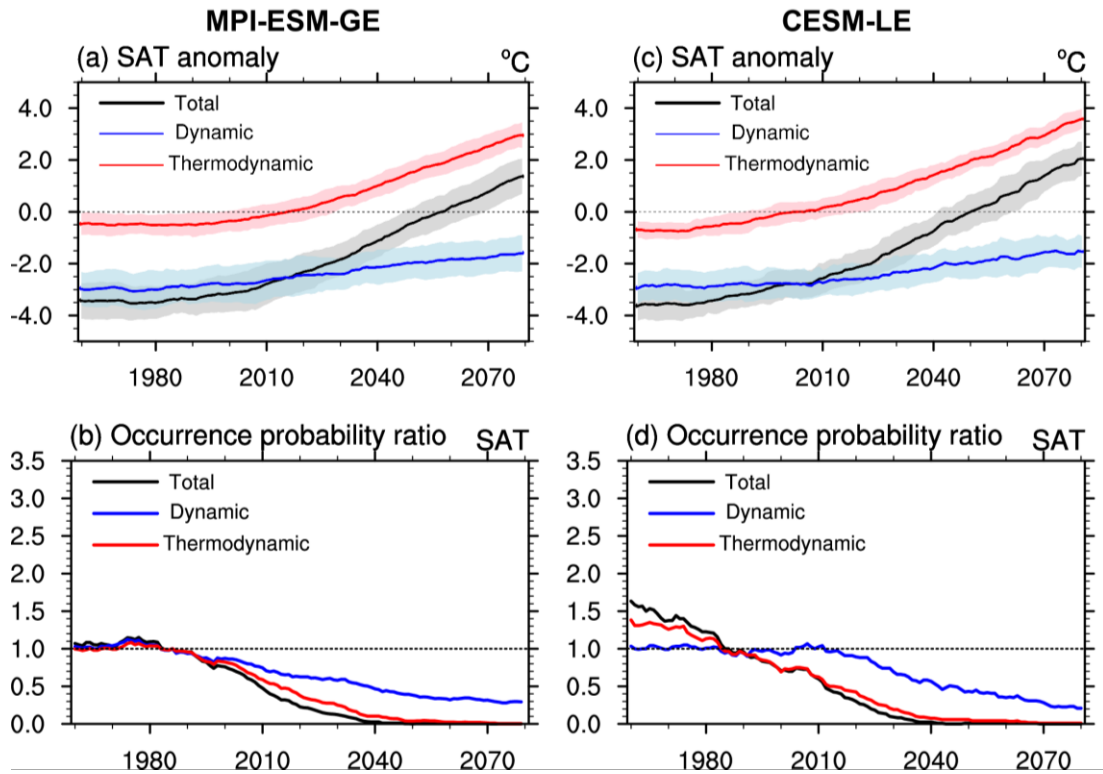
727

728 **Figure 4** (a) Time series of the 20-yr running averaged cold-month SAT anomaly (black)

729 and its dynamically-induced (blue) and thermodynamically-induced (red) components

730 over East Asia relative to the 1986-2005 boreal winter climatology in the MPI-GE. The

731 shading shows the range of two standard deviations among the model members. (b)

732 Time series of the occurrence probability ratio of the present-day East Asian cold

733 extremes in the MPI-GE: both dynamic and thermodynamic components change

734 (black), only dynamic component changes (blue) and only thermodynamic component

735 change (red). Subplots (c) and (d) correspond to subplots (a) and (b), but for the results

736 in the CESM-LE. cold months are defined as the months in which the regional mean

737 SAT is lower than the statistical 5th percentile of the climatological monthly SAT series

738 during DJF in a certain time slice.
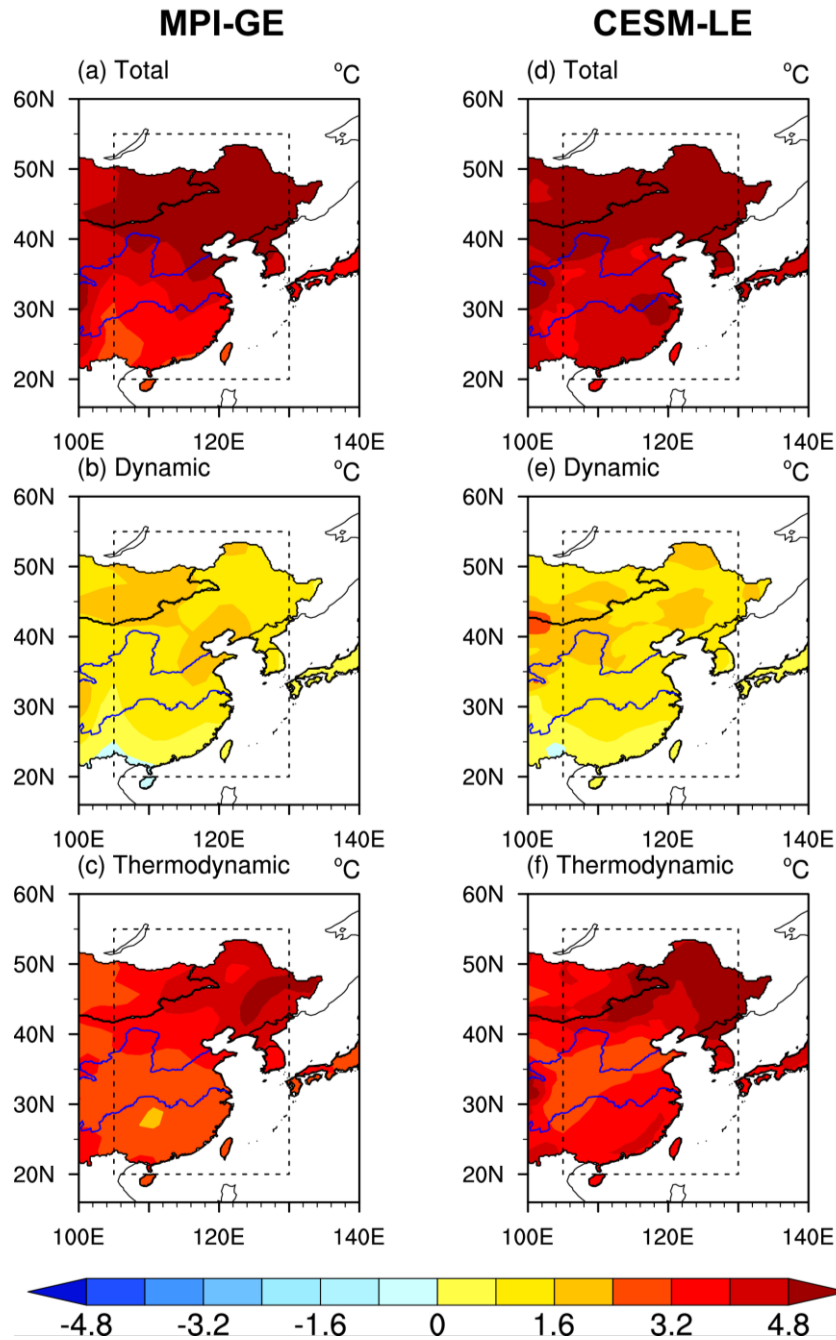
Figure 5 Changes in East Asian cold-month SAT in the MPI-GE in 2079-2098 boreal

winter relative to 1986-2005 boreal winter: (a) Total, (b) dynamic component and (c)

thermodynamic component. Subplots (d)-(f) correspond to subplots (a)-(c), but for the

results in the CESM-LE.
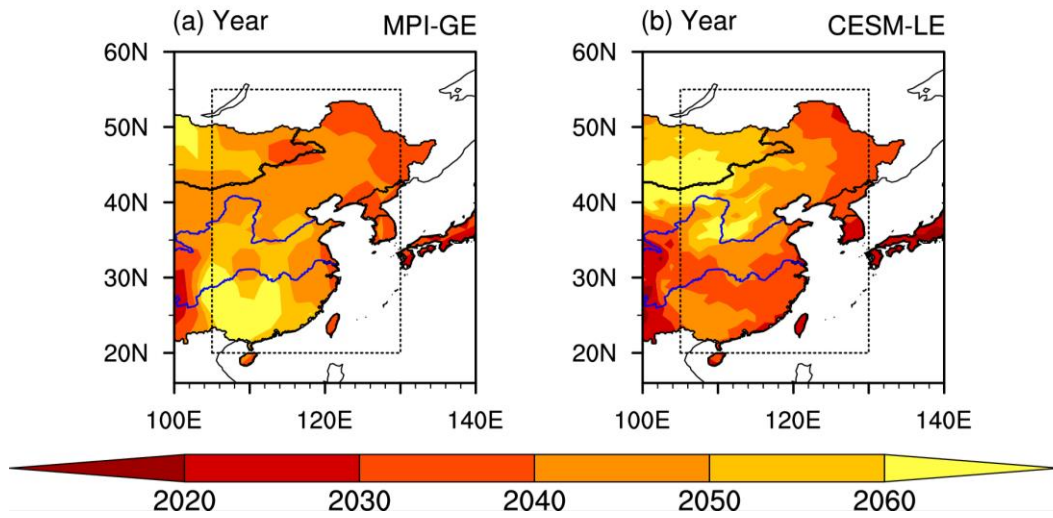
744

745 **Figure 6** The year when the occurrence probability ratio of the present-day (1986-2005

746 boreal winter) East Asian cold extremes decreases to 0.05 in (a) The MPI-GE and (b)

747 the CESM-LE.

748
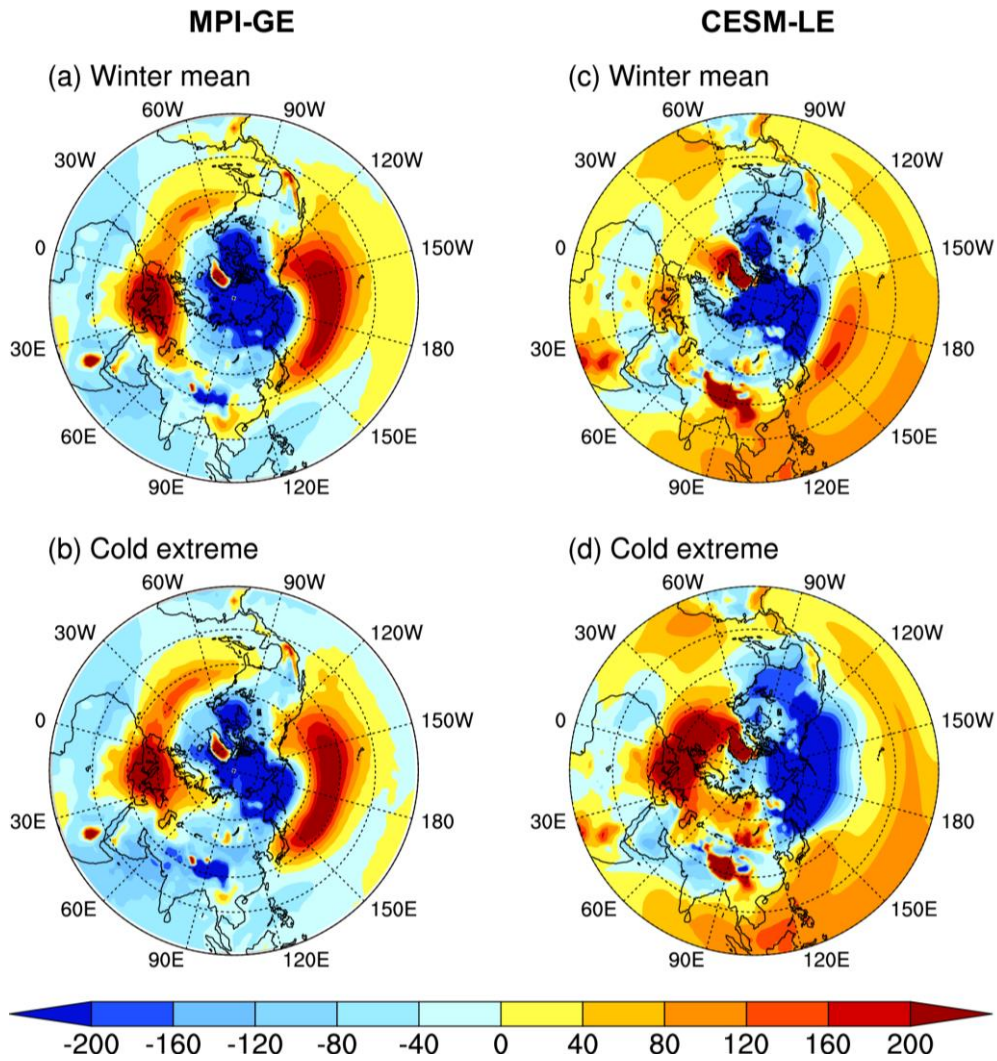
Figure 7 Changes in SLP for (a) total winter months and (b) cold months in 2079-2098

750 boreal winter relative to 1986-2005 boreal winter in the MPI-GE. Subplots (c) and (d)

751 correspond to subplots (a) and (b), but for the results in the CESM-LE.
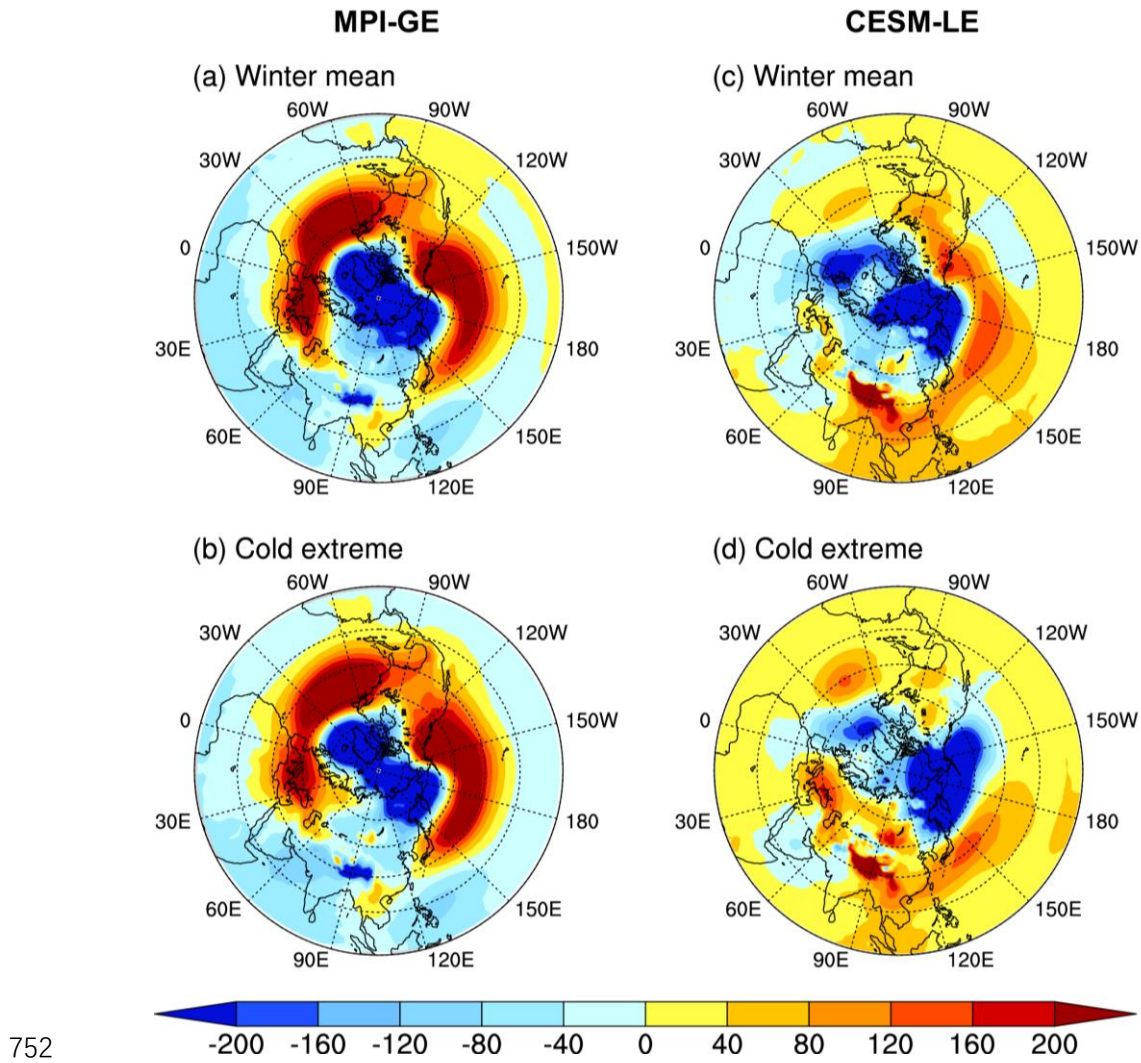
Figure 8 Changes in the dynamic component of SLP for (a) total winter months and (b) cold months in 2079-2098 boreal winter relative to 1986-2005 boreal winter in the MPI-GE. Subplots (c) and (d) correspond to subplots (a) and (b), but for the results in the CESM-LE.